PROPAGATION OF TURBULENCE INTO THERMALLY AND SALINITY STRATIFIED FLUIDS SUBJECTED TO OSCILLATING GRID TURBULENCE

Charbel Bassil
Department of Mechanical Engineering
University of Melbourne
Melbourne, VIC 3010, Australia
cbassil@student.unimelb.edu.au

Wagih Abu Rowin
Department of Mechanical Engineering
University of Melbourne
Melbourne, VIC 3010, Australia
waburowin@unimelb.edu.au

Manikandan Balasubramaniyan
Department of Mechanical Engineering
University of Melbourne
Melbourne, VIC 3010, Australia
manikandan.balasubramaniyan@unimelb.edu.au

Andrew Western
Department of Infrastructure Engineering
University of Melbourne
Melbourne, VIC 3010, Australia
a.western@unimelb.edu.au

Joseph Klewicki
Department of Mechanical Engineering
University of Melbourne
Melbourne, VIC 3010, Australia
klewicki@unimelb.edu.au

Jimmy Philip
Department of Mechanical Engineering
University of Melbourne
Melbourne, VIC 3010, Australia
jimmyp@unimelb.edu.au

ABSTRACT

Turbulent entrainment across two-layer density interfaces is investigated experimentally in oscillating grid turbulence under both thermal and salinity stratification, representing low and high Prandtl number conditions, respectively. The entrainment rate is quantified using two approaches: direct interface tracking and the method following Turner (1968). This enables a direct comparison between estimation methodologies. Interface tracking is performed using both scalar fields and vorticity-based detection, and both result in similar values of entrainment rates. Interface tracking in thermal stratification, however, exhibits consistently higher entrainment rates than salinity stratification across the full range of Richardson numbers investigated. In contrast, when using Turner (1968)'s method, the classical behaviour reported first by Turner (1968) is recovered, with comparable entrainment at low Richardson numbers and enhanced thermal entrainment at higher Richardson numbers. These results demonstrate that the observed entrainment behaviour depends strongly on the method used to quantify it, and highlight the combined influence of molecular diffusivity and measurement methodology in stratified turbulence.

INTRODUCTION

Background and Motivation

Turbulent entrainment across density interfaces is a fundamental process governing mixing in geophysical and environmental flows such as lakes, oceans, and the atmosphere. In stratified environments, the interaction between the (externally) imposed turbulence stirring the fluid and (internal) stable buoyancy resisting the vertical fluid movement, controls the rate of turbulent fluid entraining the non-turbulent fluid and mixing, affecting scalar transport and energy redistribution. Understanding the mechanisms governing entrainment is therefore essential for improving predictive models of stratified flow behaviours.

The focus of the present study is on two-layer fluids, where the top layer is of lower density (owing to higher temperature or lower salinity) than the bottom layer, and turbulence is created externally with a grid in the top layer. A key parameter characterising stratified turbulence is the Richardson number (Ri), which represents the ratio of buoyancy forces to inertial forces. Entrainment is commonly expressed through an entrainment coefficient (E), defined as the ratio of the entrainment velocity (the rate at which the turbulence or scalar in the top fluid propagates into the bottom non-turbulent region) to a characteristic velocity scale. Numerous studies have reported scaling laws of the form:

$$E \sim Ri^{-n}, \tag{1}$$

where n typically lies between 1 and $3/2$.

Role of Molecular Diffusivity

The influence of molecular diffusivity is commonly characterised by the Prandtl and Schmidt numbers, defined as

$$Pr = \frac{\nu}{\alpha} = \frac{\mu c_p}{k}, \qquad Sc = \frac{\nu}{D_s}, \tag{2}$$

where ν is the kinematic viscosity, α is the thermal diffusivity, k is the thermal conductivity, c_p is the specific heat, and D_s is the molecular diffusivity of salt in water. For the thermal cases considered here, the corresponding Prandtl number lies approximately in the range $4.5 \leq Pr \leq 6.3$. For the salinity cases, using the salt diffusivity in water at 24°C gives a Schmidt number of approximately $Sc \approx 600$. Thus, the present experiments compare moderate-*Pr* thermal stratification with high-*Sc* salinity stratification.

The influence of molecular diffusivity on entrainment has been highlighted in the classical studies of Turner (1968), which showed that thermal stratification can exhibit enhanced entrainment compared to salinity stratification under certain conditions. This behaviour was attributed to the higher diffusivity of heat, which promotes smoothing of the density interface and facilitates mixing, whereas the lower diffusivity of salt sustain sharper interfaces over longer durations.

It remains unclear, however, whether the reported diffusivity-dependent behaviour reflects a fundamental physical mechanism or is influenced by the method used to quantify entrainment.

Oscillating Grid Turbulence and Previous Studies

Oscillating grid turbulence (OGT) provides a canonical framework for studying stratified turbulence in the absence of mean shear. In this configuration, turbulence is generated by a vertically oscillating grid, allowing the effects of buoyancy to be isolated from shear-driven mechanisms.

Previous experimental studies of OGT have primarily focused on salinity as the stratifying scalar. Early experiments by Thompson & Turner (1975) examined mixing across a density interface generated by grid induced turbulence, while Xuequan & Hopfinger (1986) further explored entrainment behaviour and provided widely used datasets for *E*–*Ri* scaling. More recently, Verso *et al.* (2017) investigated entrainment in OGT using a steady-state two-layer configuration, again focusing on a salinity-stratified system.

In contrast, relatively few studies have examined thermal stratification in OGT, or directly compared heat and salt stratified interfaces under comparable conditions. Turner (1968) investigated both temperature and salinity stratification using a scalar-based approach, showing that molecular diffusivity influences entrainment at high Richardson numbers, while its effect becomes less important at low Richardson numbers. Similar behaviour was later reported by Zellouf *et al.* (2005), who used the same method as Turner (1968) and found results consistent with Turner's observations.

Despite these efforts, most experimental investigations of OGT have focused on a single scalar, typically salinity. As a result, the influence of molecular diffusivity in shear-free turbulence remains largely unexplored.

Motivation and Research Gap

While the influence of molecular diffusivity has been identified in the classical study of Turner (1968), these experiments relied primarily on scalar-based estimates of entrainment, in which the entrainment rate is inferred from the temporal rate of change of scalar (salt concentration or temperature) within the mixed layer, rather than from direct tracking of the density interface. These measurements were also constrained by the experimental techniques available at the time. Despite similar experimental configurations, the relationship between interface-based and scalar-based estimates of entrainment has not been systematically examined. This gap is particularly important, as it is unclear whether observed diffusivity-dependent behaviour arises from physical mechanisms or from the way entrainment is quantified. Herein we investigate these issues.

Present Study

The objective of the present study is to experimentally investigate entrainment in oscillating grid turbulence under both thermal and salinity stratification, representing low and high Prandtl number conditions, respectively. The entrainment coefficient E is quantified using two complementary approaches: direct tracking of the turbulent/non-turbulent interface (TNTI) position and estimation from the temporal evolution of scalar fields (i.e., the location where the scalar value is half-way between the original top and bottom values). This allows a direct comparison with classical measurements based on scalar change, as originally proposed by Turner (1968). The results are analysed over a wide range of *Ri* and compared with existing datasets, including those of Turner (1968), Xuequan & Hopfinger (1986), and Verso *et al.* (2017). The study aims to assess whether diffusivity-dependent entrainment behaviour persists, and to examine how the choice of measurement method influences the observed scaling.

EXPERIMENTAL SETUP

Oscillating Grid Tank

The experiments were conducted in an Oscillating Grid Tank (OGT) facility consisting of a double-tank configuration with inner and outer glass tanks, as shown in Figure 1. This tank follows the design of McCorquodale & Munro (2018) and Ramesh *et al.* (2024). The dimensions of the inner and outer tanks are $25 \times 25 \times 35$ cm^3 and $33 \times 33 \times 50$ cm^3, respectively, given in the order of length, width and height. The double-tank configuration minimises secondary flows and promotes near-isotropic turbulence. The grid is composed of square acrylic bars arranged orthogonally, each bar measuring $1 \times 1 \times 32$ cm^3, and the grid's mesh spacing $M = 4$ cm, as shown in the inset of Figure 1. The grid is connected to a stepper motor assembly that allows it to oscillate vertically. The frequency of the grid (f_g) is controlled by adjusting the motor speed and is varied between 1 and 3 Hz. The vertical stroke length of the grid (S) is fixed at 5.5 cm.

Thermal Stratification

In order to generate thermal stratification, a 2.5 kW immersed coil heater is used to heat the upper layer of the inner tank. The temperature of the tank is measured using ten Type-E thermocouples at a sampling frequency of 37.5 Hz through two Data Translation (DT9828) analog-to-digital converters. The thermocouples are mounted on a vertical rack and distributed from the water surface to the bottom of the inner tank with a spacing of ~ 4 cm between adjacent thermocouples.

A relay system to activate the heater is synchronised with the thermocouples to initiate measurements once the desired temperature (i.e., density) is achieved. The target temperature in the upper layer is determined based on the density ratio, which represents the strength of the stratification and is defined as follows:

$$\Delta\rho/\rho_0 = \frac{\rho_B - \rho_0}{\rho_0}, \tag{3}$$

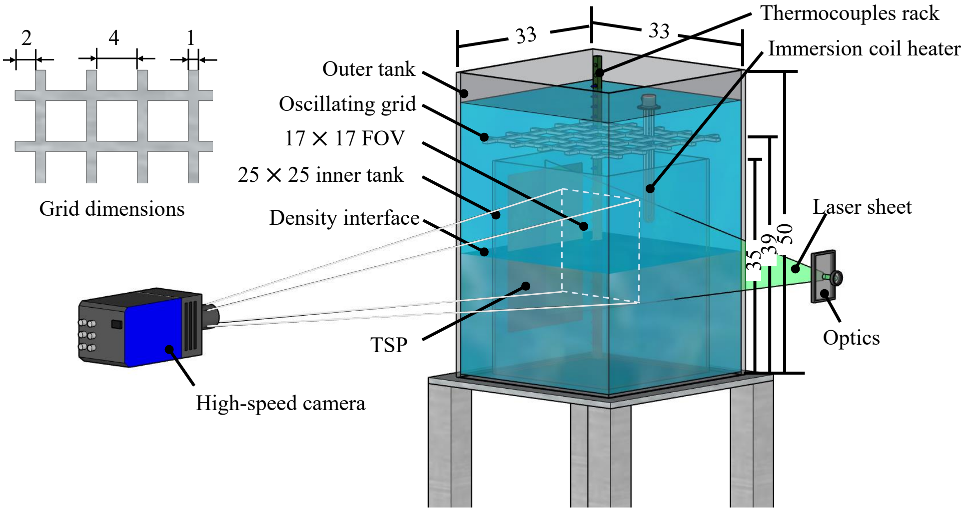

Figure 1: Schematic of the OGT setup for the thermal and salinity stratification experiments, showing the tank dimensions, the coil heater, thermocouples rack and the PIV system. The salinity configuration differs only by the absence of the heater and thermocouple array. The inset shows the grid dimensions. All dimensions are in cm.

where ρ is the water density. Here, the superscript 'B' denotes the bottom denser layer (cold water in the case of thermal stratification or saltwater in the case of salinity stratification), and '0' denotes the reference layer (i.e., hot water for the thermal stratification or freshwater for the salinity stratification).

The density of freshwater as a function of temperature is computed using a polynomial fit to standard water property data (Kell, 1975):

$$\begin{aligned}\rho(T) = {} & 999.842594 + 6.793952 \times 10^{-2} T \\ & - 9.095290 \times 10^{-3} T^2 + 1.001685 \times 10^{-4} T^3 \\ & - 1.120083 \times 10^{-6} T^4 + 6.536332 \times 10^{-9} T^5,\end{aligned} \tag{4}$$

where T is the temperature. To achieve a density ratio in the range of $\Delta\rho/\rho_0 = 0.1\%$ to 0.6% for this study, the temperature of the water in the upper layer is varied between 28 °C and 38 °C, respectively, with the cold layer kept at 24 °C.

Temperature-sensitive paint (TSP) is also implemented in the current setup to visualise the density interface and mixing process, providing a non-intrusive and cost-effective method for full-field temperature measurements (e.g., Woodmansee, 1997) The TSP used in this study is sensitive over the range of $20°\text{C} \leq T \leq 50°\text{C}$, which fully covers the range of interest in the present experiments (24°C to 38°C). The TSP covers one side of the inner tank, as shown in Figure 1. Figure 2(a) shows an example of the TSP field after the upper layer has been heated up to 36°C, while the lower layer is maintained at 24°C. The two layers are clearly separated by a density interface (visible as a yellow line) with an approximate thickness of 1.5 cm. As mixing develops, the interface is observed to move downward (see Figure 2b), and the colors progressively blend, indicating the transfer of heat from the upper layer to the lower layer.

Salinity Stratification

Salinity stratification was generated by first preparing a saltwater solution by dissolving a prescribed mass of salt into a known volume of water, allowing the target density of the lower layer to be controlled accurately. Once the salt solution

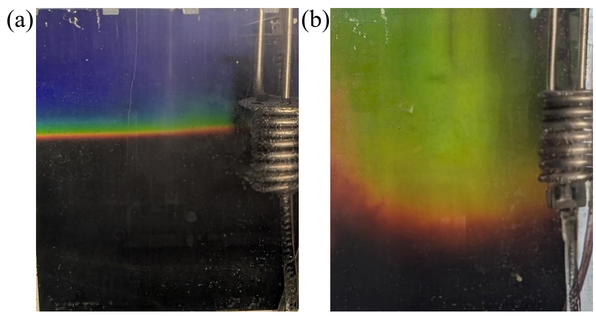

Figure 2: Sample visualisations of the TSP for the thermal stratification showing (a) the initial stratified state and (b) the mixing phase after the onset of grid oscillation (after approximately 20 minutes for the $\Delta\rho/\rho_0 = 0.35\%$ case).

is prepared, the tank is partially filled with freshwater. The saltwater is then introduced from the bottom of the inner tank using a pump and a diffuser. The pumping process is carried out carefully to minimise mixing between the two layers. As a result, the denser saltwater remains at the bottom, displacing the freshwater upward and forming a stable two-layer stratification with a sharp density interface separating the upper freshwater layer from the lower saltwater layer.

To verify the initial density profile, five sampling tubes are installed at different vertical positions along the tank wall. A small fluid sample is extracted from each height, and its density is measured using a calibrated Misco digital refractometer (PA201X-093). This procedure ensures that the desired stratification is achieved prior to the start of each experiment.

To ensure consistency between thermal and salinity experiments, the initial density profiles for representative cases with similar density ratios of $\Delta\rho/\rho_0 \approx 0.1\%$, 0.2% and 0.3% are compared in Figure 3. The temperature measurements obtained from the 10 thermocouples are used to reconstruct the initial density profile, as shown in Figure 3. At $t = 0$, the measured temperatures are converted to local density values

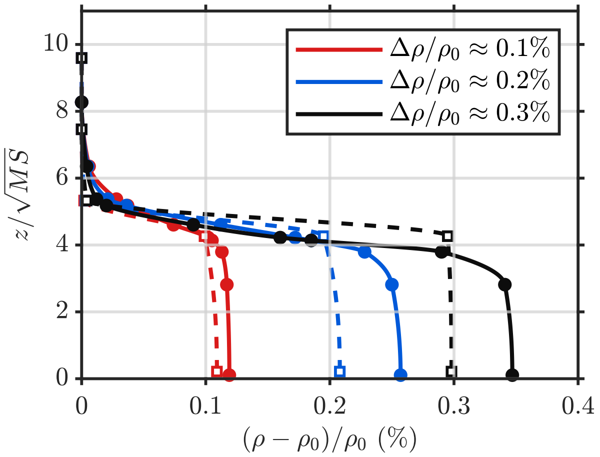

Figure 3: Initial density-ratio profiles for representative thermal and salinity stratification cases, shown as a function of the normalised vertical coordinate $z/\sqrt{MS}$. Here $z = 0$ is at the bottom of the tank. Solid and dashed lines represent thermal and salinity stratification, respectively. Symbols indicate the discrete measurement locations.

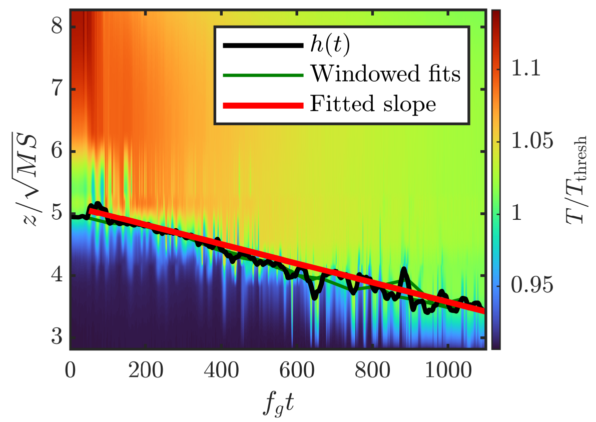

Figure 4: Thermal interface detection and entrainment estimation for Case Temp1-100. The colour map shows the normalised temperature field T/T_{thresh}. Windowed linear fits are shown in green, and the red line indicates the fitted slope.

using the equation of state (4). The resulting density field is then normalised by the reference density ρ_0, yielding the vertical profile of $(\rho-\rho_0)/\rho_0$. While both configurations exhibit a two-layer structure, small differences in the initial profiles are observed. In addition, planar laser-induced fluorescence (PLIF) was used to obtain spatially resolved measurements of salt concentration. The dye, pre-mixed in the saltwater solution, is assumed to be proportional to the salt concentration, allowing the scalar field in the field-of-view to be tracked. Details of the PLIF methodology are omitted here for brevity, as it serves as a supporting measurement.

Time-resolved PIV setup

The horizontal and vertical velocity fields for selected thermal and salinity stratification cases are measured using time-resolved PIV. In this study, the PIV data are utilised to identify the TNTI and to estimate its evolution. This approach provides an independent method to evaluate the interface evolution initially estimated from thermocouple measurements or the digital refractometer.

The PIV measurement region is confined around the density interface. The field of view (FOV) is 17 cm × 17 cm, encompassing the initial position of the density interface. Images were acquired using a high-speed PCO Dimax HS4 camera equipped with a Sigma 105 mm macro lens. The camera operated at a frame rate of 100 fps with a full resolution of 2000 × 2000 pixels, resulting in a digital resolution of 85 µm/pixel. Images were only acquired for the first 120 seconds from the start of grid oscillation.

The flow was illuminated using a dual-head Nd:YLF green laser (Photonics Industries DM2-527-50) operating at a wavelength of 527 nm with a pulse energy of 100 mJ per pulse. The laser beam of 5 mm initial diameter is passed through a collimating lens followed by a sheet-forming lens. This optical arrangement is designed to produce a uniform light sheet across the measurement plane with a thickness of ≈ 1 mm. The laser sheet is introduced from the side of the tanks, as shown in figure 1. The flow was seeded with 10 µm diameter silver-coated hollow glass spheres, which were uniformly distributed in both fluid layers prior to each experiment.

The recorded images were processed using LaVision DaVis 10.2 to obtain velocity vectors through cross-correlation analysis. The images were processed with a final interrogation window of 32 × 32 pixels, with 75% overlap, providing a spatial resolution of 2.72 mm.

Summary of Experimental Cases

Table 1 summarises the experimental conditions investigated in the present study. The cases are labelled as Salt and Temp, corresponding to salinity and thermal stratification, respectively. A total of 18 experiments were conducted, spanning density ratios in the range of 0.1% to 0.6% and grid frequencies between 1 and 3 Hz. The initial thickness of the upper layer, H, was maintained at approximately 190 mm. Of the 18 cases, some were repeated multiple times for additional data. The Richardson number Ri defined as:

$$Ri = \frac{g\,(\Delta\rho/\rho_0)\,H}{w_{\mathrm{rms}}^2}, \tag{5}$$

where g is the gravitational acceleration and w_{rms} is the root-mean-square (rms) z-component velocity induced by the oscillating grid.
To evaluate Ri, an estimate of w_{rms} is required. In oscillating grid turbulence, this velocity cannot be measured directly at the grid and is therefore estimated using the scaling proposed by Hopfinger & Toly (1976):

$$w_{rms} = f_g S \frac{\sqrt{MS}}{z'}, \tag{6}$$

where z' is the distance from a virtual origin located 1 cm below the grid mid-position. For all our cases, z' is taken to be 1 cm below the lowest position of the grid, i.e., z' = 5.5/2 - 1 = 1.75 cm.

RESULTS

Interface detection

Thermal measurements The temporal evolution of the temperature field is first examined using thermocouple data. Figure 4 shows the temperature distribution as a function of height and time for Case Temp1-100.

Table 1: Summary of experimental conditions. Cases are identified by stratification type (Salt or Temp), nominal target density ratio $\Delta\rho/\rho_0$, and grid frequency f_g. Cases marked with an asterisk (*) correspond to experiments for which PIV measurements were acquired.

Case	Ri	f_g [Hz]	$\Delta\rho/\rho_0$ (%)	Repeats
Salt1-300*	8.76	3.00	0.11	2
Salt2-300*	9.73	3.00	0.21	2
Salt3-300*	14.59	3.00	0.30	2
Salt6-300*	30.88	3.00	0.59	2
Temp1-100	64.75	1.00	0.14	3
Temp1-176	18.71	1.76	0.11	3
Temp2-176	35.62	1.76	0.22	3
Temp3-176	54.39	1.76	0.31	3
Temp1-261*	7.87	2.61	0.12	3
Temp2-261*	19.44	2.61	0.26	3
Temp3-261*	26.79	2.61	0.35	3
Temp1-200	8.09	2.00	0.08	4
Temp2-200	56.68	2.00	0.26	1
Temp3-200	40.99	2.00	0.33	2
Temp4-200	44.73	2.00	0.35	3
Temp3-150	73.43	1.50	0.33	1
Temp4-150	93.36	1.50	0.40	1
Temp5-150	111.09	1.50	0.46	1

The density interface is identified using a temperature threshold method. The threshold is defined as the average of the initial upper-layer and lower-layer temperatures. At each time step, the interface location is determined from the vertical temperature profile as the position where this threshold is reached, yielding $h(t)$. The interface position is smoothed using a moving average with a window of 2 s.

PIV-based interface detection For the PIV measurements, the TNTI is identified using a vorticity-based criterion (Mistry *et al.*, 2016). The instantaneous in-plane vorticity field is computed from the measured velocity components as:

$$\omega = -\frac{\partial w}{\partial x} + \frac{\partial u}{\partial z}. \quad (7)$$

The threshold separating turbulent and non-turbulent regions is determined using a conditional statistical approach similar to that of Mistry *et al.* (2016). An example of the detected TNTI is shown in Figure 5 overlaid on an instantaneous vorticity field from PIV measurements for Case Salt6-300.

Applying this procedure over the full time series yields the temporal evolution of the interface position. At each time instance, the z-location of the TNTI is averaged in the x-direction to obtain an instantaneous $h(t)$. The resulting signal $h(t)$ is then smoothed using a 2 s moving average to reduce high-frequency noise.

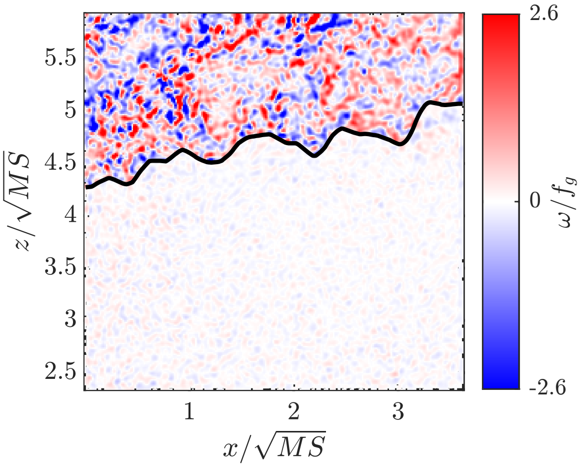

Figure 5: Instantaneous vorticity field from PIV measurements for Case Salt6-300* at t = 60 s, showing the detected TNTI.

Entrainment rate estimation

The entrainment velocity, w_e, is obtained from the temporal evolution of the interface position $h(t)$. Direct differentiation is avoided due to noise sensitivity. Therefore, a windowed linear fitting approach is applied to estimate w_e. The time series is divided into 50% overlapping windows, within which a linear fit is applied to $h(t)$ and the slope of this fit provides an estimate of the local entrainment velocity. The window duration is chosen based on temporal resolution and noise, with $\Delta t = 75$ s for thermocouple data and $\Delta t = 10$ s for PIV data. This procedure yields a set of w_e estimates as a function of time. The average of these estimates is taken as w_e for each case, as illustrated by the fitted trend in Figure 4. The entrainment velocity and rate are then defined, respectively, as:

$$w_e = \frac{\Delta h}{\Delta t}, \qquad E = \frac{w_e}{w_*}. \quad (8)$$

Using this approach, a set of (E, Ri) values is obtained for each experiment. Figure 6 shows the entrainment coefficient E as a function of the Richardson number Ri for both thermal and salinity stratification. Filled squares correspond to entrainment estimates obtained from scalar interface tracking (temperature or PLIF-based salt concentration), while open squares denote estimates based on PIV measurements. Red and blue symbols indicate thermal and salinity stratification, respectively. The scaling of the present data is also compared with the commonly reported power-law trends $E \sim Ri^{-1}$ and $E \sim Ri^{-3/2}$, shown in Figure 6. Overall, the present measurements exhibit a general agreement with these scalings, with both thermal and salinity cases following similar trends over the range of Ri investigated.

The entrainment coefficients obtained using the interface-tracking approach indicate a clear separation between thermal and salinity cases. Here the thermal cases exhibit consistently higher values of E across the entire range of Ri investigated. This behaviour is evident in Figure 6, where the present thermal measurements are systematically positioned above the corresponding salinity cases for comparable values of Ri. This indicates enhanced entrainment in thermally stratified flows when the interface evolution is used to quantify entrainment.

To facilitate comparison with previous studies, the entrainment coefficient E is also evaluated using the approach of Turner (1968). For a two-layer system of initial upper-layer

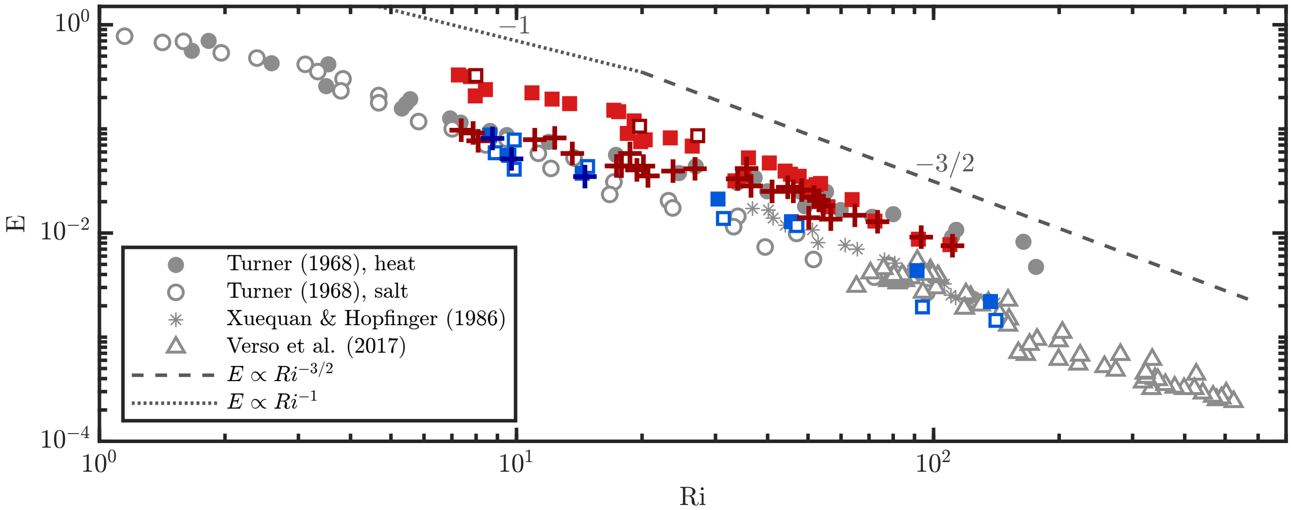

Figure 6: E as a function of Ri. The present measurements are shown using coloured markers. Red symbols correspond to thermal stratification and blue symbols to salinity stratification. Filled squares represent scalar interface-tracking estimates, while open squares represent PIV-based estimates. Estimates using Turner (1968)'s method are shown using plus symbols.

depth H and initial scalar difference $(c_2 - c_1)$ across the interface , where c_1 and c_2 denote the initial temperature or salinity in the top and bottom layer, respectively, w_e can be expressed as:

$$w_e = \frac{H}{c_2 - c_1}\frac{dc}{dt}, \tag{9}$$

where c represents the scalar value in the top layer that is mixed. In the present study, the scalar value $c(t)$ is evaluated at positions corresponding to $z/\sqrt{MS} = 6.5$ and 7.5, which lie well above the density interface and within the mixed region. The values at these locations are averaged to provide a representative estimate of the mixed-layer scalar at each time instant. This formulation links the entrainment velocity to the temporal evolution of the scalar field in the mixed layer, assuming that the layer remains well-mixed and that the interface remains sharp. Estimates using Turner (1968)'s method given by (9) are represented by plus symbols in Figure 6.

When this method is applied to the present data, the classical behaviour of Turner (1968) is recovered: thermal and salinity stratification exhibit comparable E at low Ri, while thermal stratification shows enhanced E at higher Ri.

DISCUSSION AND CONCLUSION

The present study demonstrates a systematic difference in entrainment behaviour between thermal and salinity stratification in OGT. Using the interface-tracking approach, thermal cases consistently exhibit higher entrainment rates than salinity cases across the full range of Richardson numbers investigated. However, when the entrainment rate is evaluated according to the method of Turner (1968) using (9), the results of Turner (1968) are recovered, with comparable entrainment at low Richardson numbers and enhanced thermal entrainment at higher Richardson numbers.

This discrepancy highlights the influence of the measurement methodology on the observed entrainment behaviour. The interface-tracking approach quantifies the advancement of the density interface, whereas Turner (1968)'s method reflects both entrainment and the subsequent mixing within the turbulent layer. As a result, the method of Turner (1968) may underestimate entrainment at lower Richardson numbers, where the interface can advance more rapidly than the scalar field homogenises.

These findings suggest that part of the diffusivity-dependent behaviour reported in Turner (1968) may be influenced by the measurement approach rather than solely by the underlying physical mechanisms. Overall, the present results demonstrate that both molecular diffusivity and measurement methodology play a key role in determining entrainment behaviour in stratified turbulence.

ACKNOWLEDGEMENT

The authors thank the Australian Research Council for the financial support. C. Bassil acknowledges financial support from the University of Melbourne through the Graduate Research Scholarship for his PhD study.

REFERENCES

Hopfinger, EJ & Toly, J-A 1976 *J. Fluid Mech.* **78** (1), 155–175.

Kell, George S. 1975 *J. Chem. Eng. Data* **20** (1), 97–105.

McCorquodale, M & Munro, RJ 2018 *Exp. Fluids* **59** (12), 182.

Mistry, D, Philip, J, Dawson, J & Marusic, I 2016 *J. Fluid Mech.* **802**, 690–725.

Ramesh, B, Klewicki, J & Philip, J 2024 *Exp. Fluids* **65** (4), 46.

Thompson, SM & Turner, JS 1975 *J. Fluid Mech.* **67** (2), 349–368.

Turner, JS 1968 *J. Fluid Mech.* **33** (4), 639–656.

Verso, L, van Reeuwijk, M & Liberzon, A 2017 *Phys. Rev. Fluids* **2** (10), 104605.

Woodmansee, MA 1997 PhD thesis, University of Illinois at Urbana-Champaign.

Xuequan, E & Hopfinger, EJ 1986 *J. Fluid Mech.* **166**, 227–244.

Zellouf, Y, Dupont, P & Peerhossaini, H 2005 *Int. J. Heat Mass Transf.* **48** (18), 3722–3735.